Supplemental Information to Manuscript:

Prevention of hypoxia by myoglobin expression in human tumor cells promotes differentiation and inhibits metastasis

Maria Galluzzo, Selma Pennacchietti, Stefania Rosano, Paolo M. Comoglio, and Paolo Michieli

Laboratory of Experimental Therapy, Institute for Cancer Research and Treatment (IRCC), University of Turin Medical School, I-10060 Candiolo, Turin, Italy

Supplemental Methods

In vitro biochemical and biological assays

Growth rate analysis was performed as described (1). The percentage of dead cells was determined on exponentially growing cells using trypan blue (Sigma, St. Louis, Missouri). Apoptosis was determined by the free nucleosome method using the Cell Death Detection ELISA^{PLUS} kit (Boehringer, Mannheim, Germany) according to the manufacturer's instructions. DNA synthesis was measured by BrdU incorporation using the Cell Proliferation ELISA chemoluminescence kit (Boehringer). Intracellular ATP levels were analyzed using the Cell Titer-Glo Luminescent Cell Viability Assay kit (Promega, Madison, Wisconsin). Lactate production was assayed in the conditioned medium using a specific kit (BioVision, Mountain View, California). Oxygen consumption was determined using a Clark-type oxygen electrode as described (2). For HIF-1α induction, lentiviral-vector transduced cells were incubated at different pO_2 values (21%, 3%, 1% or 0.1%) for 3 hours, and HIF-1α levels were determined by Western blotting (on nuclear extracts) using anti-HIF-1α antibodies (BD Transduction Laboratories, San Jose, California). Alternatively, cells were subjected to repeated cycles of hypoxia and re-oxygenation (1 hour at 21%, 3%, 1% or 0.1% O_2 followed by 30 minutes at 21% O_2, repeated 3 times), and HIF-1α levels were determined by Western blotting. Cells incubated at 21% O_2 were used as controls. Collagen-embedded tumor spheroids were obtained as described (3). Spheroids were incubated in normoxia (21% O_2) for 24 hours; following addition of 0.25 mM pimonidazole hydrochloride (Chemicon, Temecula, California), they were further incubated for 24 hours at 5% O_2 and then formalin fixed, embedded in paraffin and processed for histological analysis. Intracellular hypoxia was determined on serial sections using the Hypoxyprobe kit (Chemicon)

according to the manufacturer's instructions. ROS levels were determined using carboxy-dihydro-dichloro-diacetyl-fluorescine (c-H_2DCFDA; Molecular Probes, Eugene, Oregon) as described (3). Briefly, lentiviral vector-transduced cells expressing wild-type or mutant Mb were incubated with c-H_2DCFDA for 30 minutes. Following probe uptake, cells were stimulated with increasing concentrations (1-100 μM) of H_2O_2, and fluorescence emission was determined after 1 hour using a DTX 800 Multimode Detector (Beckman Coulter, Fullerton, California). Data were normalized using the oxidized form of the same probe (c-DCFDA; Molecular Probes). Scavenging activity is expressed as % of the fluorescence delta between the treated and untreated control (empty vector). NO scavenging assays were performed as described (5). Briefly, cells were pre-incubated with c-H_2DCFDA as above, and then stimulated with increasing concentrations (0.1-1.0 mM) of S-nitroso-N-acetyl-DL-penicillamine (SNAP; Sigma). Fluorescence emission was determined after 1 hour as above.

Experimental metastasis analysis

For pulmonary experimental metastasis analysis, lentiviral vector-transduced A549 lung carcinoma cells were injected ($1 \cdot 10^6$ cells/mouse) into the tail vein of six-week old immuno-deficient *nu/nu* female mice on Swiss CD-1 background (6 mice/group; Charles River, Lecco, Italy). After one month, mice were euthanized and lungs were frozen in liquid nitrogen for DNA extraction. For abdominal experimental metastasis analysis, lentiviral vector-transduced FG-2 pancreatic carcinoma cells ($2 \cdot 10^5$ cells/mouse) were injected intraperitoneally into six-week old immuno-deficient *nu/nu* female mice on Swiss CD-1 background (6 mice/group; Charles River). After one month, mice were euthanized and autopsied for the presence of metastatic lesions in the peritoneal cavity. Experimental metastases were scored using a stereoscopic microscope.

Tissue analysis and real time PCR

Expression of Mb in tumors was determined by immuno-histochemistry using a monoclonal anti-FLAG antibody (Sigma). Immuno-histochemical analysis with Hypoxyprobe monoclonal antibodies (Chemicon) was performed on paraffin-embedded tumor sections according to the manufacturer's instructions. Analysis of HIF-1α expression was determined on frozen sections by immuno-fluorescence analysis as described (6). Expression of CAIX was analyzed by immuno-histochemistry using an anti-human CAIX antibody (M75; a gift of Silvia Pastorekova, Bratislava University, Slovakia). Immuno-fluorescence analysis of tumor vessels was performed on frozen sections using anti-PECAM-1 (CD31 endothelial marker) rat monoclonal antibody (Pharmingen, San Diego, California). Histological analysis was performed on paraffin-embedded sections stained with hematoxylin and eosin or PAS/Alcian. Tumor proliferation was determined using a monoclonal anti-Ki67 antibody as previously described (MIB1; 7). Apoptosis was evaluated on frozen sections with a TUNEL reaction using an In Situ Cell Death Detection Kit (Roche, Basel, Switzerland). Metastases were detected by immuno-histochemistry on paraffin-embedded lung sections using rabbit polyclonal anti-GFP antibodies (Molecular Probes). Quantification of *gfp* gene content in lung genomic DNA was performed by TaqMan analysis as described (1). Frozen lungs were processed for genomic DNA extraction using a Blood & Cell Culture DNA kit (Qiagen, Valencia, California). Lung genomic DNA was amplified using an ABI Prism 7700 analyzer (Applied Biosystems, Foster City, California) according to the protocol suggested by the manufacturer. The following oligonucleotides were used as primers: 5' AGCAAAGACCCCAACGAGAA 3' (sense); 5' GGCGGCGGTCACGAA 3' (antisense). The Taqman probe used for real time PCR had the following sequence: 5' CGCGATCACATGGTCCTGCTGG 3'. Normalization of *gfp* signal was performed as described

(8). The $\Delta\Delta C_T$ value was calculated by subtracting the ΔC_T obtained analyzing lung genomic DNA from a tumor-free mouse to the individual ΔC_T of each sample.

Direct measurement of intratumoral pO_2

Intratumoral pO_2 was determined by the fluorescence quenching method (9) using an OxyLab pO_2 tissue oxygenation monitoring system with a NP/O/E pO_2 needle-type sensor (Oxford Optronix, Oxford, United Kingdom). This technique exploits the ability of O_2 in solution to quench fluorescence emitted by a ruthenium probe. An optical fiber that ends with the probe is connected to a multi-channel module. Fluorescence emitted by the probe is inversely proportional to the concentration of oxygen around the probe and to the temperature. The fiber transmits the emitted light to the module, and the module calculates the pO_2 value that is displayed on a LCD monitor. Temperature is entered manually. Mice bearing experimental tumors were anesthesized using a combination of Zoletil (30 mg/kg; Virbac, Milano, Italy) and Xylor (5 mg/kg; Bio98, Milano, Italy). Using a 23G needle, a 'track' was created through the tumor. After a few minutes, the needle-type ruthenium probe was fully inserted into the track so that the tip was just 1 or 2 mm from the opposite surface of the tumor. Following pO_2 measurement, the probe was retracted by approximately 2 mm and oxygen concentration was measured again, and so forth for the entire length of the track. On average, each tumor was measured along 2 distinct tracks and each track provided 3 different measurements, for a total of 6 points per mouse. Since mechanical stress induces transient changes in local tissue oxygenation, each measurement was protracted for approximately 10-15 minutes to allow the pO_2 value to stabilize. The same procedure was employed to determine control, subcutaneous pO_2 values on the opposite, tumorless mouse flank.

Statistical analysis

Statistical significance was determined using a two-tail homoscedastic Student's t-Test (array 1, control group; array 2, experimental group; n = 3-36 depending on the experiment). For all data analyzed, a significance threshold of $p < 0.05$ was assumed. In all figures and tables, values are expressed as mean ± standard deviation (unless differently stated), and statistical significance is indicated by a single ($p < 0.05$) or double ($p < 0.01$) asterisk above the bar. The data generated *in vitro* are representative of at least two distinct experiments conducted in triplicate. In the experiments conducted *in vivo* at least 6 mice per group were employed. Tissue analysis was conducted on at least 6 different fields per sample.

References

1. Mazzone, M., Basilico, C., Cavassa, S., Pennacchietti, S., Risio, M., Naldini, L., Comoglio, P.M., and Michieli, P. 2004. An uncleavable form of pro-scatter factor suppresses tumor growth and dissemination in mice. *J. Clin. Invest.* **114**:1418-1432.
2. Papandreou, I., Cairns, R.A., Fontana, L., Lim, A.L., and Denko, N.C. 2006. HIF-1 mediates adaptation to hypoxia by actively downregulating mitochondrial oxygen consumption. *Cell Metab.* **3**:187-197.
3. Meyer, M., Clauss, M., Lepple-Wienhues, A., Waltenberger, J., Augustin, H.G., Ziche, M., Lanz, C., Buttner, M., Rziha, H.J., and Dehio, C. 1999. A novel vascular endothelial growth factor encoded by Orf virus, VEGF-E, mediates angiogenesis via signalling through VEGFR-2 (KDR) but not VEGFR-1 (Flt-1) receptor tyrosine kinases. *EMBO J.* **18**:363-374.
4. Moeller, B.J., Cao, Y., Li, C.Y., and Dewhirst, M.W. 2004. Radiation activates HIF-1 to regulate vascular radiosensitivity in tumors: role of reoxygenation, free radicals, and stress granules. *Cancer Cell* **5**:429-441.
5. Gunasekar, P.G., Kanthasamy, A.G., Borowitz, J.L., and Isom, G.E. 1995. Monitoring intracellular nitric oxide formation by dichlorofluorescin in neuronal cells. *J. Neurosci Methods* **61**:15-21.
6. Pennacchietti, S., Michieli, P., Galluzzo, M., Mazzone, M., Giordano, S., and Comoglio, P.M. 2003. Hypoxia promotes invasive growth by transcriptional activation of the met protooncogene. *Cancer Cell* **3**:347-361.
7. Ellis, P.A., Smith, I.E., Detre, S., Burton, S.A., Salter, J., A'Hern, R., Walsh, G., Johnston, S.R., and Dowsett, M. 1998. Reduced apoptosis and proliferation and increased Bcl-2 in residual breast cancer following preoperative chemotherapy. *Breast Cancer Res.* Treat. **48**:107-116.
8. Livak, K.J., and Schmittgen, T.D. 2001. Analysis of relative gene expression data using real-time quantitative PCR and the $2^{-\Delta\Delta CT}$ Method. *Methods* **25**:402-408.
9. Griffiths, J.R., and Robinson, S.P. 1999. The OxyLite: a fibre-optic oxygen sensor. *Br. J. Radiol.* **72**, 627-630.

Supplemental Tables

Supplemental Table 1. Wild-type myoglobin expression inhibits spontaneous but not experimental metastasis. Lentiviral vector-transduced cells were injected underneath the epidermis (MDA-MB-435-HGF melanoma cells), into the mammary fat pad (TSA mammary carcinoma cells), into the peritoneal cavity (FG-2 pancreatic carcinoma cells), and into the tail vein (A549 lung carcinoma cells). Tumor latency is the time required by injected cells to give rise to a palpable tumor (MDA-MB-435-HGF and A549 only). Metastases are quantified by TaqMan analysis of *gfp* gene content in lung genomic DNA (MDA-MB-435-HGF and A549) or by stereoscopic microscopy (TSA and FG-2). For more detailed information please refer to the Methods and Supplemental Methods sections. HE7A/HF8A Mb, His F8 Ala/His E7 Ala double mutant; N/A, not applicable; N/D, not determined.

Tumor cell type, injection site and mouse strain	Lentiviral vector	Median tumor latency (days)	Mean no. of metastases	*gfp* DNA in lungs ($2^{-\Delta\Delta CT}$)
MDA-MB-435-HGF human melanoma cells injected underneath the skin of CD-1 *nu/nu* mice	Empty vector	8	N/D	8.9 ± 2.4
	Wild-type Mb	12	N/D	2.2 ± 0.7
	HE7A/HF8A Mb	6	N/D	11.5 ± 2.3
TSA mouse breast carcinoma cells injected into the mammary fat pad of Balb-c mice	Empty vector	8	3.9 ± 1.5	N/D
	Wild-type Mb	12	0.6 ± 0.4	N/D
	HE7A/HF8A Mb	8	6.5 ± 2.3	N/D
FG-2 human pancreatic carcinoma cells injected into the peritoneal cavity of CD-1 *nu/nu* mice	Empty vector	N/A	21 ± 6.9	N/D
	Wild-type Mb	N/A	22 ± 3.6	N/D
	HE7A/HF8A Mb	N/A	28.8 ± 5.3	N/D
A549 human lung carcinoma cells injected into the tail vein of CD-1 *nu/nu* mice	Empty vector	N/A	N/D	61.5 ± 8.4
	Wild-type Mb	N/A	N/D	66.4 ± 7.1
	HE7A/HF8A Mb	N/A	N/D	87.9 ± 19.5

Supplemental Figure Legends

Supplemental Figure 1. Myoglobin expression does not alter the growth and survival of cancer cells in vitro. (A) GFP-expressing A549 human lung carcinoma cells were transduced with a lentiviral vector expressing FLAG-tagged Mb or with an empty vector as control. Mb expression was determined by Western blot (WB) analysis using anti-Mb antibodies and anti-FLAG antibodies. Mouse skeletal muscle (mSM) and mouse heart (mHT) protein extracts were used as controls. Ectopically expressed Mb (Mb-FLAG) migrates differently than endogenous Mb (Mb) due to the presence of the FLAG epitope. The bands with an apparent molecular mass similar to that of mouse Mb in lanes 3 and 4 result from a non-specific reaction of the secondary antibody with A549 protein extracts. A549 EV, A549 cells transduced with empty vector; A549 Mb, A549 cells expressing ectopic Mb; kDa, kilo-Dalton. (B) The growth rate of lentiviral vector-transduced cells was measured in the presence of 2% FBS. (C) Cell viability and apoptosis were determined by trypan blue count and free nucleosome analysis, respectively. A.U., arbitrary units; EV, empty vector. (D) DNA synthesis was determined by BrdU incorporation in the presence or absence of serum growth factors.

Supplemental Figure 2. Myoglobin expression promotes oxygenation of tumor-like spheroids. (A) Lentiviral vector-transduced cells were seeded in a 3D Matrigel layer and allowed to form tumor-like spheroids in a normoxic environment (21% O_2). Two representative microscopic fields per group are shown. BF, bright field. Magnification: 100X. (B) Following addition of the hypoxia-specific probe pimonidazole hydrochloride, spheroids were incubated in mild hypoxia (5% O_2), and then processed for histological analysis. Spheroid sections were

analyzed by immuno-histochemistry using anti-pimonidazole antibodies and counter-stained with Mayer's hematoxylin. Ten representative microscopic fields per group are shown. PIMO, pimonidazole. Magnification: 400X.

Supplemental Figure 3. Myoglobin expression results in lower HIF-1α levels. (A) HIF-1α levels were determined by immuno-fluorescence analysis of tumor sections using anti-human HIF-1α antibodies (green). Nuclei are stained with DAPI (blue). Magnification: 200X. The number of HIF-1α-positive cells per microscopic field analyzed is indicated in parenthesis (mean ± sd). (B) Immuno-histochemical analysis of tumor sections using anti-CAIX antibodies. CAIX (Carbonic Anhydrase IX) is a HIF-1-regulated hypoxia marker. Magnification: 50X.

Supplemental Figure 4. Myoglobin expression reduces tumor cell proliferation and death. (A) Proliferation index was determined by immuno-histochemical analysis of tumor sections using anti-Ki67 antibodies. (B) Apoptotic index was determined by immuno-fluorescence analysis of frozen tumor sections using the TUNEL reaction. (C) Representative images of the experiments shown in A and B. Row 1: the nucleus of proliferating cells is stained in brown. Row 2: apoptotic cells are red; nuclei are stained with DAPI (blue). Magnification: 200X.

Supplemental Figure 5. Constitutive HIF-1α expression bypasses Mb-mediated tumor suppression. (A) Western blot analysis of lentiviral vector-transduced A549 cells using anti-HIF-1α antibodies (on nuclear extracts) and anti-FLAG antibodies (on total lysates). Mut. HIF, P402A/P564A HIF-1α mutant. (B) Analysis of experimental tumor burden approximately five weeks after subcutaneous tumor cell injection. Statistical significance is calculated between each experimental group and the control group (empty vector). (C) Analysis of tumor angiogenesis.

Microvascular density (MVD) is the number of CD31-positive vessels per square mm of tumor section. Statistical significance as in B. (D) Analysis of spontaneous pulmonary metastases. The extent of lung colonization by GFP-positive cancer cells was determined by Taqman analysis of lung genomic DNA. Values are expressed as $2^{-\Delta\Delta CT}$ using lung genomic DNA from a tumor-free mouse as reference sample. Statistical significance as in B and C. (E) Histological analysis of tumor sections stained with hematoxylin and eosin (H&E). One representative image per experimental group is shown. Magnification: 100X.

Supplemental Figure 6. Mutant Mb displays enhanced free radical scavenging activity compared to wild-type Mb. (A) Cell-based ROS scavenging assay. Lentiviral-vector transduced cells were incubated with 100 μm H_2O_2 for 1 hour and ROS levels were determined by fluorescence. Scavenging activity is expressed as % relative to the delta between untreated and treated control. Statistical significance is calculated between each experimental group and the untreated empty vector group. EV, empty vector; WT, wild-type Mb; HF8Y, HisF8Tyr Mb; HE7A HF8A, HisE7Ala/HisF8Ala Mb. (B) Cell-based NO scavenging assay. Lentiviral-vector transduced cells were incubated with 1 mM SNAP for 1 hour and NO levels were determined by fluorescence. Data expression and statistical significance as in A.

Supplemental Figure 1

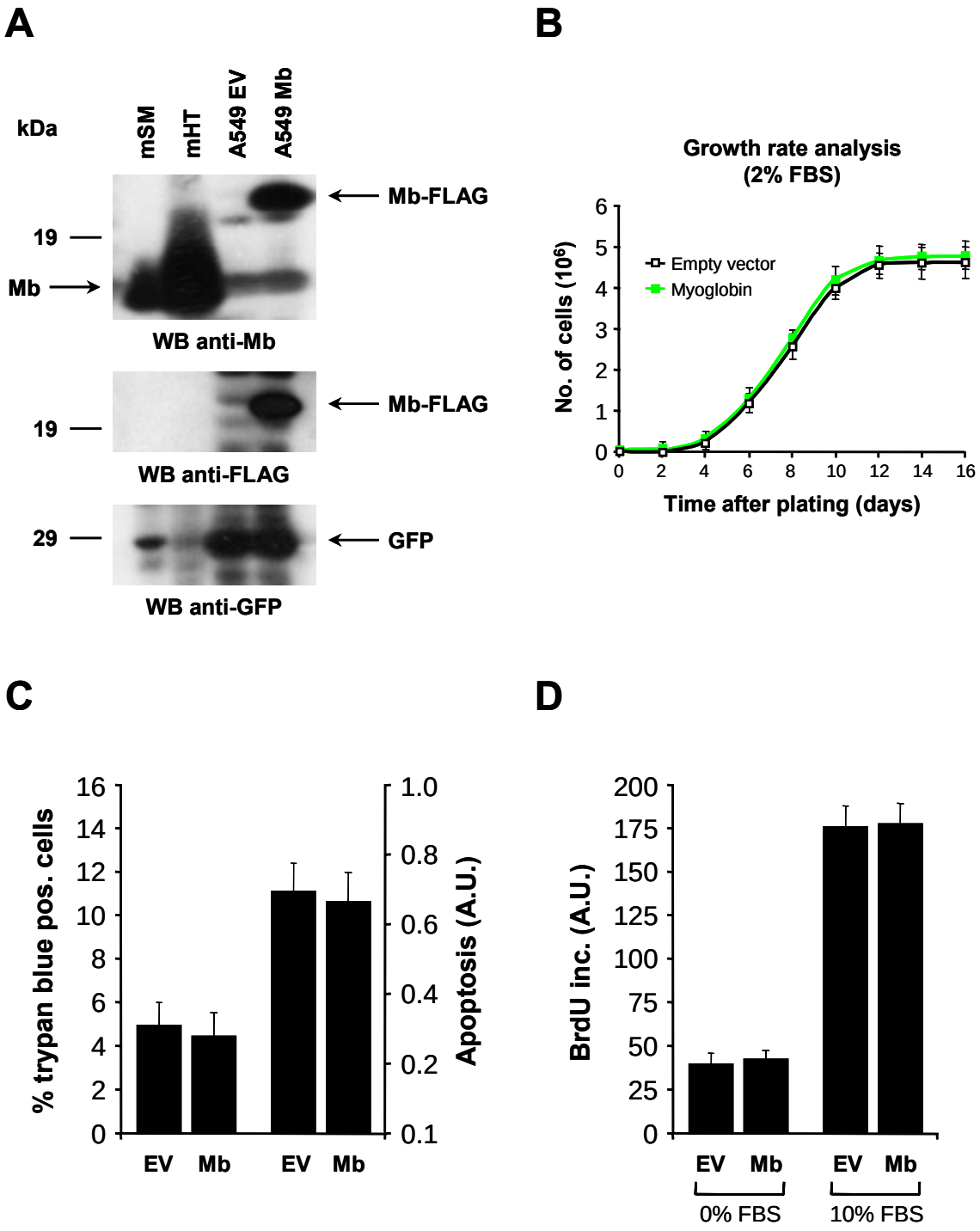

Supplemental Figure 2

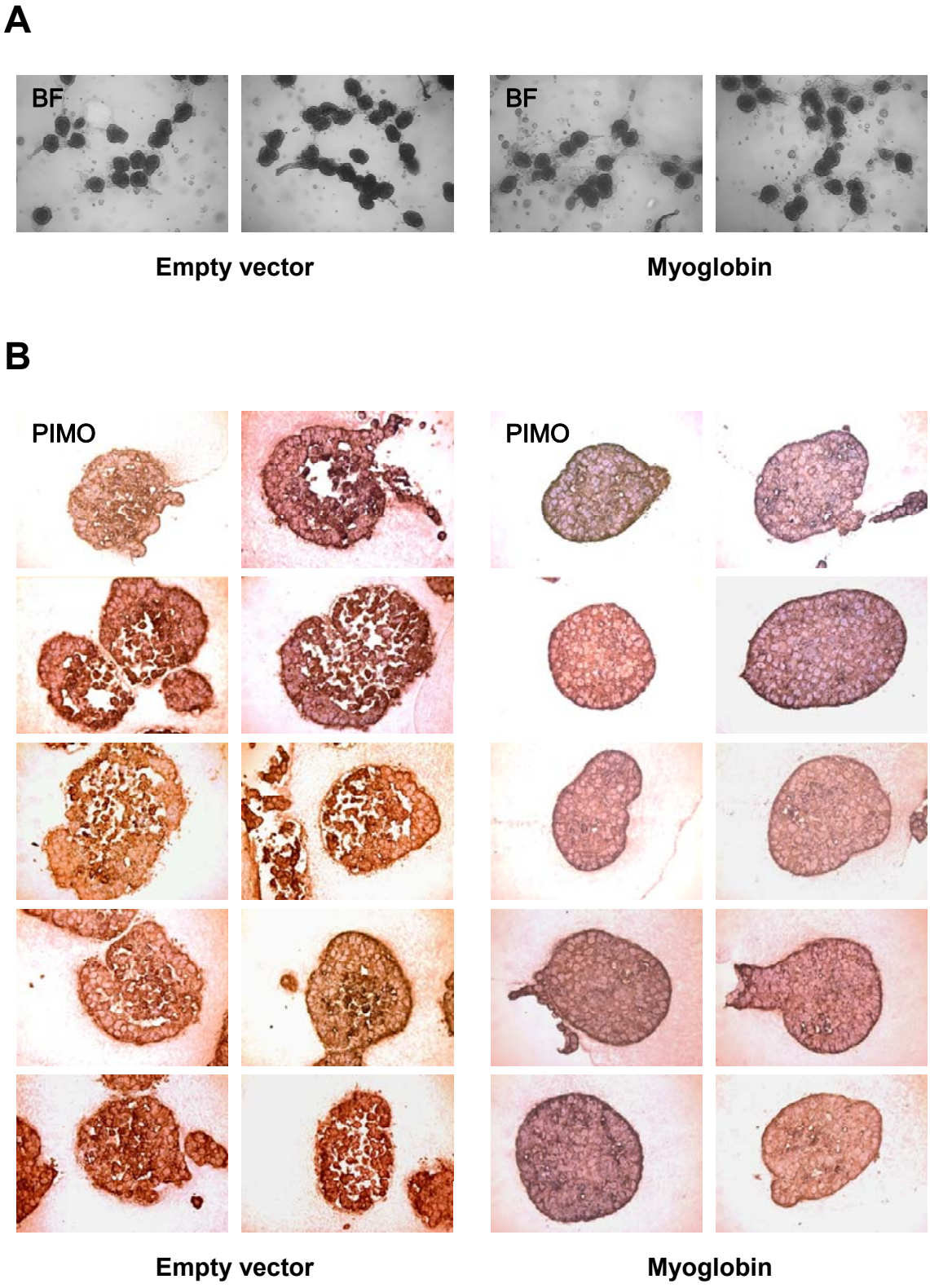

Supplemental Figure 3

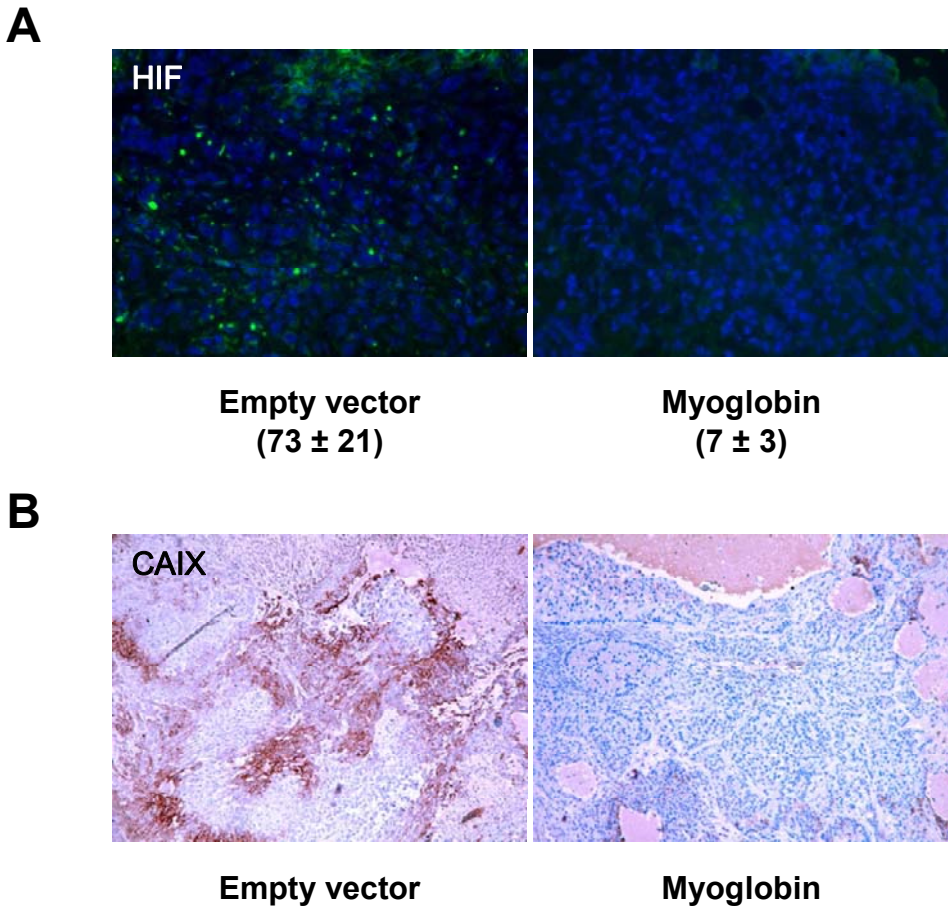

Supplemental Figure 4

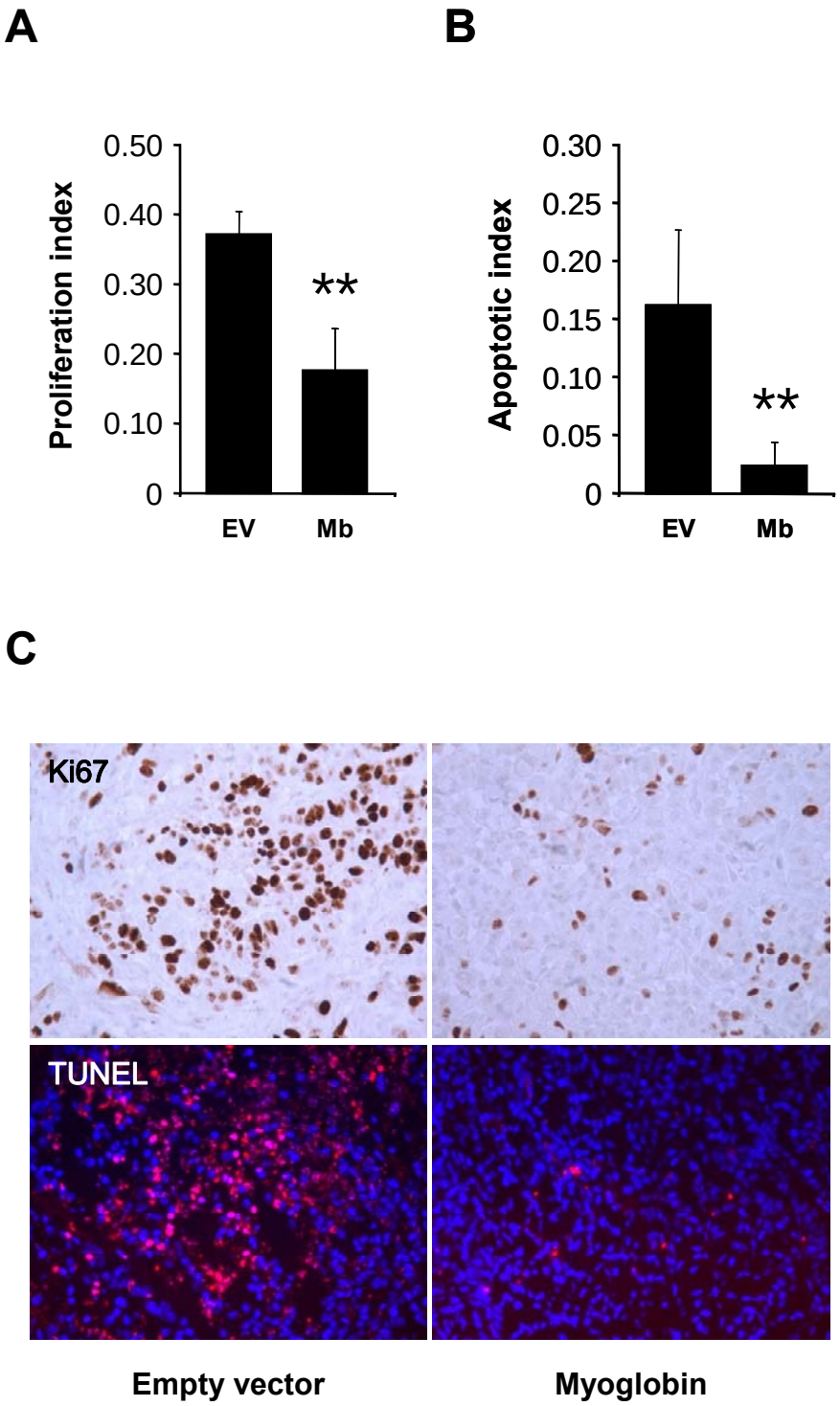

Supplemental Figure 5

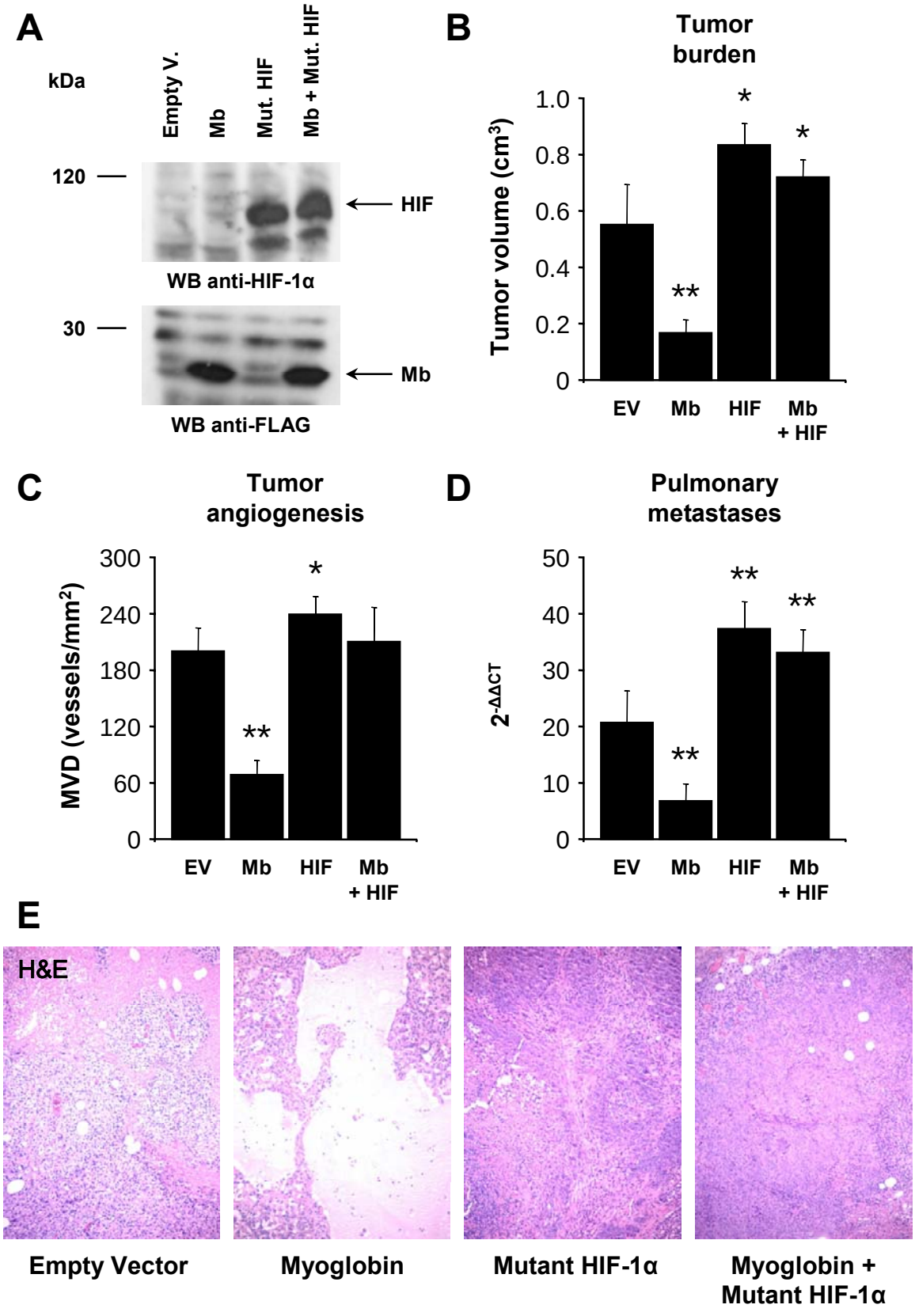

Supplemental Figure 6